Tunable Four-wave Mixing Light Source Based on Photonic Crystal Fibers with Variable Chromatic Dispersion

Lorena Velázquez-Ibarra, Antonio Díez, Enrique Silvestre, and Miguel V. Andrés

***Abstract*— We present a detailed experimental study of four-wave mixing tuning in photonic crystal fibers that were filled either with ethanol or with heavy water. It is demonstrated that wide tuning ranges can be achieved in both cases through the variable chromatic dispersion generated by thermo-optic effect. Tunability of the signal band from 745 nm to 919 nm, and of the idler band from 1260 nm to 1759 nm is demonstrated with a pump at 1064 nm. Numerical calculations were carried out and show good agreement with experimental measurements.**

***Index Terms*— Photonic crystal fibers, Nonlinear optics, Four-wave mixing, nonlinear microscopy.**

I. Introduction

Four-wave mixing (FWM) is a well-known optical nonlinear effect arising from the third-order susceptibility that can cause the generation of new frequencies when one (or two) intense optical signal interacts with a nonlinear medium such as an optical fiber [1]. Several all-optical fiber devices that rely on FWM, such as wavelength converters, parametric amplifiers, optical demultiplexers, chromatic dispersion compensators, etc., have been demonstrated in the past. Moreover, the specific properties of FWM in optical fibers have been also exploited for the development of new light sources with emission characteristics suited for certain specific applications such as, for example, correlated photon-pair generation [2], and coherent anti-Stokes Raman scattering (CARS) microscopy [3-5].

As four-wave mixing is a phase-sensitive process, i.e. the interaction depends on the relative phases of the beams, its effect can efficiently accumulate over long distances along the fiber when a phase-matching condition is satisfied. This requires that the chromatic dispersion profile of the fiber has a suitable shape. In this context, the advent of the photonic crystal fiber (PCF) technology allowed for the first time an unprecedented control of dispersion and nonlinear characteristics of optical fibers. The development of light sources based on FWM generation in PCFs has meant a highly valuable contribution that impacts significantly on the development of user-friendly, robust, all-fiber sources that would make optical technologies readily available for applications [6, 7].

PCFs are special optical fibers whose cross-section is formed by a periodic array of air holes with dimensions of the order of micrometers. The dispersion profile of these fibers is highly dependent on the geometrical parameters of their microstructure, air-hole diameter d and pitch Λ, which makes them very attractive for dispersion engineering [8-10]. However, once the fiber is fabricated with the proper choice of parameters, its optical properties are fixed. Propagation properties of PCFs can be further expanded by filling the air-holes with proper materials, which can lead to some new applications. Many different substances such as liquids [11], liquid crystals [12], gases [13], and polymers [14] among others, have been used in the past to add capabilities and/or to enhance the fiber's performance. In some cases, dynamic tuning of fiber properties is achieved with filling materials whose physical properties are influenced by external physical magnitudes [15].

Optical fibers with tunable chromatic dispersion can be notably useful to applications where nonlinear effects need to be exploited in a flexible and dynamic way. For instance, in the particular case of CARS microscopy, the ability to tune the FWM bands allows matching the vibrational frequencies of different molecules of interest, which allows imaging different molecular species with the same light source [16]. The wider the FWM tuning range, the larger is the set of molecules that can be addressed.

Over the last years, different mechanisms have been exploited to tune the dispersion of a PCF, and hence, the nonlinear effects that can be generated in it [17]. Infiltration of different materials inside the air holes of a PCF can greatly enhance the flexibility of these fibers when the refractive index of those materials is tuned through different mechanisms like temperature, stress or external electric fields [18,19].

In a previous work [20], we reported preliminary experimental results regarding the tunability of FWM bands in a photonic crystal fiber infiltrated with ethanol. Wide tuning of the FWM generated bands was demonstrated by tuning the dispersion properties of the infiltrated fiber through temperature. Here, we complement the results presented in [20] with a full experimental study of this effect investigated in a range of PCFs with different structural parameters and dispersion properties. We also investigated the use of different

L. Velázquez is with Departamento de Física, Universidad de Guanajuato (Mexico) and with Departamento de Física Aplicada y Electromagnetsimo - ICMUV, Universidad de Valencia (Spain). e-mail: lorenav@fisica.ugto.mx

A. Díez, and M.V. Andrés are with Departamento de Física Aplicada y Electromagnetsimo - ICMUV, Universidad de Valencia (Spain).

E. Silvestre is with Departamento de Óptica - ICMUV, Universidad de Valencia (Spain).

Manuscript received XXX; revised August YYY.

liquids with suitable refractive index and thermal properties for this specific application. We report in the present work experimental results on FWM thermal tuning in heavy water filled PCFs.

II. Principle of Operation

Degenerate four-wave mixing is a phase-sensitive process, meaning that its efficiency is ruled by a phase-matching condition, given by

$$2\beta(\omega_p) = \beta(\omega_i) + \beta(\omega_s) + 2\gamma P \quad (1)$$

where β is the propagation factor of the fiber mode, ω_p, ω_s, and ω_i are the angular frequencies of the pump, signal and idler fields respectively, γ is the nonlinear coefficient of the fiber, and P is the pump power. The frequencies of the parametric bands are determined by Eq. (1) together with conservation of energy. Eq. (1) indicates that the parametric wavelength of Stokes and Anti-Stokes generated photons depends on the dispersion properties of the fiber. Thus, changes in the propagation factor can lead to the shift of the parametric bands. The thermo-optic effect can be used to tune the dispersion properties of liquid-infiltrated PCFs by thermally inducing a change in the refractive index of the liquid that fills the holes of the fiber.

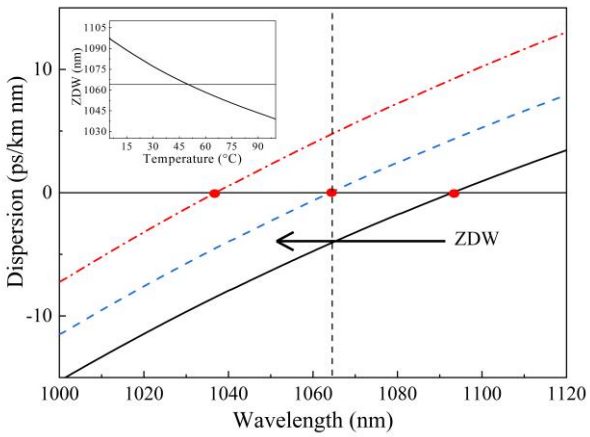

Fig. 1. Dispersion curves for an ethanol-infiltrated PCF at different temperatures: $T = 5\ ^\circ$C (black solid line), $T = 45\ ^\circ$C (blue dashed line) and $T = 100\ ^\circ$C (red dash-dot line). The dashed vertical line indicates a 1064 nm pump. Inset: ZDW as a function of temperature. Fiber structural parameters: $\Lambda = 3.3$ µm, $d/\Lambda = 0.88$.

Figure 1 shows an example of the dispersion profile of a PCF infiltrated with ethanol, for three temperatures: 5 ºC, 45 ºC and 100 ºC. Calculations were done using a fully vectorial method (FVM) [21]. We have assumed a linear dependence of the refractive index of the liquid, n, on the temperature change, $\Delta T = T - T_0$,

$$n(\Delta T) = n_0 + \frac{dn}{dT}\Delta T \quad (2)$$

where n_0 is the refractive index of the liquid at T_0=20 ºC, and dn/dT is its thermo-optic coefficient (TOC). The chromatic dispersion of the PCF increases at any wavelength, and the zero-dispersion wavelength (ZDW) shifts toward shorter wavelengths with the increase of temperature; this is expected for a liquid with a negative TOC, as it was considered in the calculations. For this specific PCF, the dispersion at 1064 nm switches from normal to anomalous at a temperature of 50 ºC. The inset of Fig. 1 shows the ZDW as a function of temperature.

Figure 2 (a) shows the parametric phase-matching wavelengths as a function of pump wavelength for the fiber and temperatures considered in Fig. 1. The phase-matching curves change with temperature accordingly with the shift of dispersion. For this specific PCF, no FWM effect is expected to be generated below T = 15 °C for a pump of 1064 nm. For larger temperatures, theoretical calculations show that FWM bands will be generated at that pump wavelength, with parametric wavelengths approaching the pump wavelength as the temperature increases. This behavior is summarized in Fig 2(b) where the parametric wavelengths are shown as a function of temperature for a pump wavelength of 1064 nm. Within the range of temperatures addressed in Fig 2 (b), the bands' shift is not linear with temperature, and an important change of shift rate happens when the dispersion of the fiber changes from normal to anomalous. Significant bands' shifts are feasible provided that the fiber is properly designed. A wavelength shift of around 255 nm for the signal band and 637 nm for the idler band is predicted within an 80 ºC temperature change for this specific PCF. In general terms, the tuning range and tuning rate depends on both, the properties of the liquid, i.e. refractive index and TOC, but also on the dispersion properties of the fiber which, in the last instance, depend on its structural parameters.

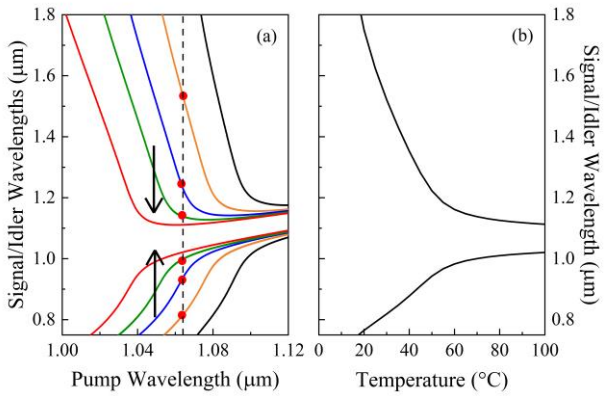

Fig. 2. (a) Phase-matching curves calculated for the ethanol-infiltrated PCF at different temperatures: T = 5 ºC (black), T = 25 ºC (orange), T = 45 ºC (blue), T = 65 ºC (green) and T = 100 ºC (red). Peak pump power used in the calculations: P = 350 W (average power of 5 mW). The dashed vertical line indicates a 1064 nm pump. (b) Phase-matching wavelengths as a function of temperature.

III. PCF Design and Fabrication

The PCFs used in this work were designed to have the appropriate chromatic dispersion profile to generate widely-spaced FWM bands at the experimental pump wavelength of

1064 nm when the holes were filled with the corresponding liquid. The generation of widely-spaced FWM bands requires the fiber dispersion at the pump wavelength to be normal and small, with the ZDW close to the pump wavelength. Ethanol and heavy water were selected to infiltrate the PCFs, based on their thermo-optic coefficient, refractive index, absorption and viscosity. Specifically, heavy water was preferred against regular deionized (DI) water because of the deep absorption bands that DI water exhibits in the near infrared. The Sellmeier coefficients for these liquids as reported in [22] were used in the calculations.

The fibers were fabricated following the stack-and-draw technique. The geometrical parameters (pitch Λ and hole diameter to pitch ratio d/Λ) were measured from scanning electron microscope (SEM) images for each fiber; they are summarized in Table I. PCF-1, PCF-2 and PCF-3 were infiltrated with ethanol, and PCF-4 with heavy water. An SEM image of PCF-4 is shown as an inset in Fig. 4.

The dispersion of the fibers before and after infiltration is quite different. The calculated chromatic dispersion for two of the fabricated PCFs with air and liquid in the holes are shown in Fig. 3 (a). The ZDW of the PCFs before infiltration is located far below the pump wavelength; it redshifts when the refractive index of the holes is increased from air to the refractive index of the liquid, as a result of the decrease in numerical aperture. The calculated ZDW for the PCFs with air and with liquid at room temperature are reported in Table I. Figure 3 (b) shows the calculated ZDW change with temperature for all four PCFs. For these calculations, the TOC values assumed were -3.99×10^{-4} ºC^{-1} for ethanol [23], and -6.6×10^{-5} ºC^{-1} for heavy water [24]. The contribution of silica to the thermal response of the infiltrated fibers was neglected since silica's TOC, 8.6×10^{-6} ºC^{-1} [25], is almost one order of magnitude lower than that of the studied liquids. For simplicity, the wavelength dependence of the TOCs was neglected in this work. It has been reported that TOC of ethanol and water changes linearly with wavelength [26]. Taking it into account will introduce a slight correction to the phase-matching wavelengths calculated in this work.

As it has been already indicated in the previous section, the ZDW shifts to shorter wavelengths as the temperature increases. The shift rate is larger in the case of fibers filled with ethanol than in fibers filled with heavy water, in line with the corresponding TOC values. As an example, at room temperature, the ZDW shift rates for each fiber are 773 pm/°C (PCF-1), 695 pm/°C (PCF-2), 591 pm/°C (PCF-3), and 106 pm/°C (PCF-4). It is worth remarking that the shift rate is approximately between 5 and 36 times larger than the one reported for an empty PCF [17].

TABLE I
CALCULATED ZDW BEFORE AND AFTER INFILTRATION

Fiber	Λ(μm)	d/ Λ	ZDW (nm)	
			AIR	LIQUID
PCF-1[a]	3.2	0.70	937	1104
PCF-2[a]	3.3	0.70	938	1098
PCF-3[a]	3.8	0.82	925	1075
PCF-4[b]	2.7	0.60	939	1072

[a] Fiber filled with ethanol
[b] Fiber filled with heavy water

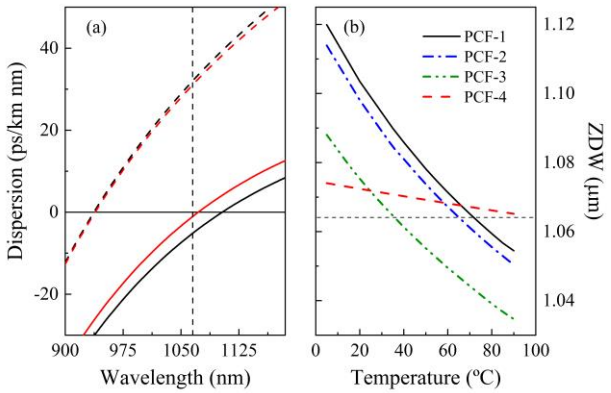

Fig. 3. (a) Chromatic dispersion as a function of wavelength for PCF-1: filled with air (black dashed line) and ethanol (black solid line); and PCF-4: filled with air (red dashed line) and heavy water (red solid line) at room temperature. The dashed vertical line indicates the experimental pump wavelength. (b) Calculated ZDW as a function of temperature for all PCFs; the dashed horizontal line indicates the experimental pump wavelength.

VI. EXPERIMENTAL RESULTS

Fiber sections with lengths between 75 cm and 100 cm were pressure-infiltrated with ethanol (PCF-1, 2, 3) and with heavy water (PCF-4). After the infiltration process, the PCFs were fusion spliced to a single-mode fiber (SMF) at the input (injection fiber) and to a multi-mode fiber (MMF) at the output (collection fiber). This served two principal purposes: it helped prevent the evaporation of the liquid during the experiments, and it allowed the whole PCF section to be immersed in a thermal bath providing temperature uniformity along its length.

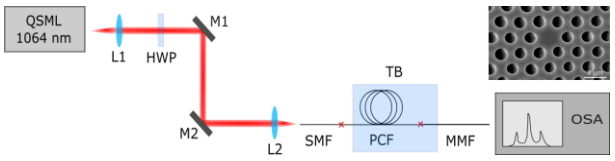

Fig. 4. Experimental setup used to tune the FWM wavelengths: (QSML) Q- switched microchip laser, (L) lens, (M) mirror, (HWP) half-wave plate, (TB) thermal bath, (OSA) optical spectrum analyzer.

The experimental setup is schematically shown in Fig. 4. A Nd:YAG Q-switched microchip laser (QSML) emitting at 1064 nm (0.72 ns pulses, repetition rate of 19.9 kHz) was used to pump the fibers, which were immersed in a thermal bath to allow control over the temperature of the fiber. To reduce bending losses as much as possible, the radius of curvature of the fiber coil within the thermal bath was kept as large as possible, typically about 15 cm. To investigate the effects of temperature on the FWM generation, the temperature T of the thermal bath was varied in a range between 7 ºC and 90 ºC. Output spectra were recorded for different temperatures with an optical spectrum analyzer (OSA).

The spectra obtained at different temperatures with (a) PCF-3 and (b) PCF-4 are shown in Fig. 5. In both cases,

FWM bands shift towards the pump wavelength with increasing temperatures, as it has been anticipated in the previous section. Changes in the refractive index of the liquid caused by the temperature changes, resulted in changes in the effective mode area, which had an impact on the amplitude of the generated FWM bands. The amplitude of the FWM bands increases with increasing temperature as it is expected since the refractive index for a liquid with negative TOC decreases with increasing temperature, thus, reducing the effective area and the confinement loss. To compensate this effect, the pump power launched into the fiber was regulated in each measurement by readjusting the light launching conditions to keep the amplitude of the FWM bands constant. The average pump power used in the experiments ranges between 17 mW and 60 mW measured at the output of the MMF; these values correspond to peak pump powers between 1.2 kW and 4.2 kW.

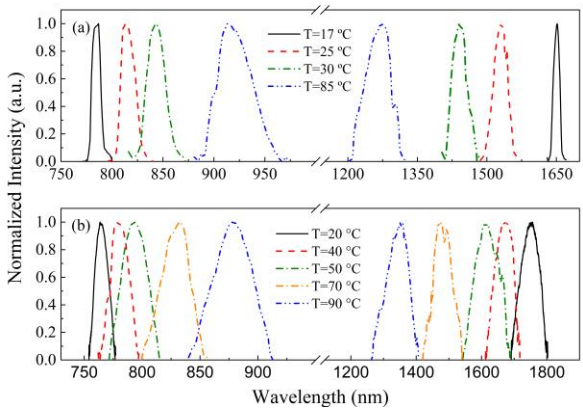

Fig. 5. FWM signal and idler bands obtained at different temperatures for (a) PCF-3 infiltrated with ethanol and (b) PCF-4 infiltrated with heavy water.

The evolution of the central wavelength of the FWM bands with temperature is summarized in Fig. 6 for all the fibers. The studied temperature range differs for each fiber depending on their properties; e.g., no FWM bands were observed at room temperature in PCF-1 and PCF-2, however they were generated in PCF-4; in the case of PCF-3 the FWM bands were observed even below room temperature. Within the investigated temperature range, the bands of the fibers infiltrated with ethanol show a wavelength shift from 745 nm to 919 nm for the signal band and from 1260 nm to 1677 nm for the idler band. In the case of PCF-4 filled with heavy water, a wavelength shift from 764 nm to 877 nm was obtained for the signal band, and from 1349 nm to 1759 nm for the idler band.

V. Discussion

The dependence of FWM wavelengths with temperature was studied theoretically for the different PCFs. The phase-matching curves at the experimental pump wavelength were calculated for different temperatures using the propagation factors provided by the FVM [21]. Changes of the effective area of the optical beams caused by changes of refractive index due to temperature were taken into account. The nonlinear refractive index used for the calculations was $n_2 = 2.7\times10^{-20}$ $W^{-1}m^2$, which is the commonly used n_2 of silica. The contributions of the liquids to the nonlinearity were neglected in the calculations since the overlapping between the optical beam and the holes is minor.

Numerical simulations with different values of Λ and d/Λ around the ones obtained from the SEM images (Table I) were performed. The numerical simulations results that best agree with experimental results are included in Fig. 6. Table II summarizes the fiber structural parameters that provided the best fit between modelling results and experiment, together with the relative difference with respect to the SEM parameters. Although a more accurate theoretical modelling can be performed, for example, by including the wavelength dispersion of the TOCs, and the liquids' nonlinearity, in general terms, we can conclude that the experimental results are well described by the theoretical simulations. The agreement between the fiber structural parameters obtained from SEM images and the parameters used for theoretical modelling is reasonably good. Notice that the fiber structural parameters taken from the SEM images are affected by the accuracy of the SEM scale.

TABLE II
BEST-FIT FIBER PARAMETERS

Fiber	Λ(μm)	RD[a] (%)	d/ Λ	RD[a] (%)
PCF-1[a]	3.0	6	0.78	11
PCF-2[a]	3.0	9	0.77	10
PCF-3[a]	3.3	13	0.91	11
PCF-4[b]	2.7	0	0.66	10

[a]RD: relative difference with respect to SEM measured values

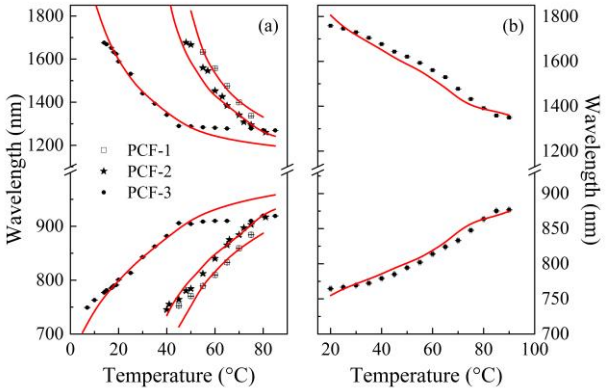

Fig. 6. Experimental (scatter) and calculated (solid line) signal and idler wavelengths for different PCFs infiltrated with (a) ethanol, and (b) heavy water.

Finally, we would like to make a comment on the convenience of using either ethanol or heavy water. Heavy water has a smaller TOC than ethanol, which causes that the thermal tuning rate of FWM bands to be smaller than in the case of ethanol, as it was shown here. However, we can point out some advantages of using heavy water against ethanol that can make its use more convenient in some cases. Firstly, the light absorption of heavy water in the wavelength range of interest is lower than that of ethanol [22]. Secondly, heavy water has a lower refractive index than ethanol. Thus,

infiltrated fibers with heavy water show a rather high refractive index contrast between the holes area and the silica matrix, which contributes to lowering the fiber confinement loss. Both facts contribute to having a better guidance in the infiltrated fibers. Additionally, although the tuning rate may be lower, the achievable tuning range is comparable in both cases.

VI. Conclusions

The thermo-optic effect in liquid-filled PCFs is a practical way to obtain variable chromatic dispersion fibers with a tunable ZDW. Here, we have experimentally studied the thermo-optic effect on widely spaced four-wave mixing bands. Two different liquids were investigated: ethanol and heavy water. Even though heavy water has a smaller thermo-optic coefficient than ethanol, the wavelength tuning range that can be obtained when using heavy water can still be considerably wide. In our experiments with ethanol-filled fibers, the widest tuning range achieved was 174 nm and 417 nm for the signal and idler bands, respectively, within a temperature variation of 78 ºC. In the case of the fiber filled with heavy water, wavelength shifts of 113 nm and 410 nm for the two bands is demonstrated with a temperature variation of 70 ºC. Experimental results are compared with numerical calculations with good agreement. Our results demonstrate the potential of this approach to prepare robust and practical light sources for CARS applications.

Acknowledgment

The authors would like to acknowledge the financial support received from the Ministerio de Economía y Competitividad (MINECO) and Fonds Européen de Développement Économique et Régional (FEDER) (TEC2016-76664-C2-1-R), CONACyT (grant 250888) and PRODEP (grant 511-6/18-8876-215391).

References

[1] G. Agrawal, *Nonlinear Fiber Optics*, 5th Edition, Optics and Photonics, Academic Press, 2013.

[2] O. Alibart, J. Fulconis, G.K.L. Wong, S.G. Murdoch, W.J. Wadsworth and J.G. Rarity, "Photon pair generation using four-wave mixing in a microstructured fibre: theory versus experiment," *New J. Phys.*, vol. 8, no. 67, 2006.

[3] S. Lefrancois, D. Fu, G.R. Holtom, L. Kong, W.J. Wadsworth, P. Schneider, R. Herda, A. Zach, X.S. Xie, and F.W. Wise, "Fiber four-wave mixing source for coherent anti-Stokes Raman scattering microscopy," *Opt. Lett*., vol. 37, no. 10, pp. 1652-1654, 2012.

[4] M. Baumgartl, T. Gottschall, J. Abreu-Afonso, A. Díez, T. Meyer, B. Dietzek, M. Rothhardt, J. Popp, J. Limpert, and A. Tu¨nnermann, "Alignment-free, all-spliced fiber laser source for cars microscopy based on four-wave-mixing," *Opt. Express*, vol. 20, no. 19, pp. 21010–21018, 2012.

[5] T. Gottschall, T. Meyer, M. Baumgartl, B. Dietzek, J. Popp, J. Limpert, and A. Tu¨nnermann, "Fiber-based optical parametric oscillator for high resolution coherent anti-stokes raman scattering (CARS) microscopy," *Opt. Express*, vol. 22, no. 18, pp. 21 921–21 928, 2014.

[6] M. Chemnitz, M. Baumgartl, T. Meyer, C. Jauregui, B. Dietzek, J. Popp, J. Limpert, and A. Tunnermann, "Widely tuneable fiber optical parametric amplifier for coherent anti-Stokes Raman scattering microscopy," Opt. Exp., vol.20, no. 24, pp. 26583-26595, 2012.

[7] G. Wong, A. H. Chen, S. Murdoch, R. Leonhardt, J. Harvey, N. Joly, J. Knight, W. Wadsworth, and P. Russell, "Continuous-wave tunable optical parametric generation in a photonic-crystal fiber," *J. Opt. Soc. Am. B*, vol. 22, no. 11, pp. 2505–2511, 2005.

[8] T. Birks, D. Mogilevtsev, J. Knight, and P. Russell, "Dispersion compensation using single-material fibers," *Phot. Tech. Lett.*, vol. 11, no. 6, pp. 674–676, 1999.

[9] K. Saitoh, M. Koshiba, T. Hasegawa, and E. Sasaoka, "Chromatic dispersion control in photonic crystal fibers: application to ultra-flattened dispersion," *Opt. Exp.*, vol. 11, no. 8, pp. 843–852, 2003.

[10] A. Zheltikov, "Nanomanaging dispersion, nonlinearity, and gain of photonic-crystal fibers," *Appl. Phys. B*, vol. 84, no. 1-2, pp. 69–74, 2006.

[11] Boris T. Kuhlmey, Benjamin J. Eggleton, and Darran K. C. Wu, "Fluid-filled solid-core photonic bandgap fibers," J. Lightwave Technol., vol. 27, no. 11, pp. 1617-1630 (2009).

[12] T. T. Larsen, A. Bjarklev, D. S. Hermann, and J. Broeng, "Optical devices based on liquid crystal photonic bandgap fibres," Opt. Express 11, pp. 2589-2596 (2003).

[13] F. Benabid, F. Couny, J. C. Knight, T. A. Birks & P. St J. Russell "Compact, stable and efficient all-fibre gas cells using hollow-core photonic crystal fibres" Nature, vol. 434, pp. 488-491 (2005).

[14] C. Markos, G, Antonopoulos, and George Kakarantzas, "Broadband guidance in a hollow-core photonic crystal fiber with polymer-filled cladding", IEEE Photon. Technol. Lett., vol. 25 , no. 20 , pp. 2003-2006 (2013).

[15] Y. Huang, Y. Wang, L. Zhang, Y. Shao, F. Zhang, C. Liao, and Y. Wang, "Tunable electro-optical modulator based on a photonic crystal fiber selectively filled with liquid crystal," J. Lightwave Technol., vol. 37, no. 9, pp. 1903-1908 (2019).

[16] T. Gottschall, T. Meyer, M. Baumgartl, C. Jauregui, M. Schmitt, J. Popp, J. Limpert, and A. Tu¨nnermann, "Fiber-based light sources for biomedical applications of coherent anti-stokes Raman scattering microscopy," *Laser & Photonics Reviews*, vol. 9, no. 5, pp. 435–451, 2015.

[17] J. Abreu-Afonso, A. Dez, J. L. Cruz, and M. V. Andrs, "Effects of temperature and axial strain on four-wave mixing parametric frequencies in microstructured optical fibers pumped in the normal dispersion regime," *Photonics*, vol. 1, no. 4, p. 404, 2014.

[18] M.H. Frosz, A. Stefani, and O. Bang, "Highly sensitive and simple method for refractive index sensing of liquids in microstructured optical fibers using four-wave mixing," *Opt. Express*, vol. 19, no. 1, pp. 10471–10484, 2011.

[19] M. Wahle and H. Kitzerow, "Electrically tunable zero dispersion wavelengths in photonic crystal fibers filled with a dual frequency addressable liquid crystal," *Appl. Phys. Lett.*, vol. 107, no. 20, 2015.

[20] L. Velázquez-Ibarra, A. Díez, E. Silvestre, and M. V. Andrés, "Wideband tuning of four-wave mixing in solid-core liquid-filled photonic crystal fibers," *Opt. Lett.*, vol. 41, no. 11, pp. 2600–2603, 2016.

[21] E. Silvestre, T. Pinheiro-Ortega, P. Andrés, J. J. Miret, and A. Ortigosa-Blanch, "Analytical evaluation of chromatic dispersion in photonic crystal fibers," *Opt. Lett.*, vol. 30, no. 5, pp. 453–455, 2005.

[22] S. Kedenburg, M. Vieweg, T. Gissibl, and H. Giessen, "Linear refractive index and absorption measurements of nonlinear optical liquids in the visible and near-infrared spectral region," *Opt. Mat. Exp.*, vol. 2, no. 11, pp. 1588–1611, 2012.

[23] R. Kamikawachi, I. Abe, A. Paterno, H. Kalinowski, M. Muller, J. Pinto, and J. Fabris, "Determination of thermo-optic coefficient in liquids with fiber bragg grating refractometer," *Opt. Comm.*, vol. 281, no. 4, pp. 621–625, 2008.

[24] G. Peterson, "5. Dye Lasers," in *Quantum Electronics*, Methods in Experimental Physics, Ed. C.L. Tang, Academic Press, vol. 15, Part A, pp. 251–359, 1979.

[25] D. B. Leviton and B.J. Frey, "Temperature-dependent absolute refractive index measurements of synthetic fused silica," NASA Goddard Space Flight Center, Tech. Rep. arXiv:0805.0091, 2008.

[26] Cheng-Ling Lee, Hsuan-Yu Ho, Jheng-Hong Gu, Tung-Yuan Yeh, and Chung-Hao Tseng, "Dual hollow core fiber-based Fabry–Perot interferometer for measuring the thermo-optic coefficients of liquids," Opt. Lett., vol. 40, no. 4, pp. 459-462 (2015).